



PREDICTION OF DIFFERENTIAL DRYING SHRINKAGE IN CONCRETE

J.-K. Kim¹ and C.-S. Lee

Department of Civil Engineering, Korea Advanced Institute of Science and Technology,
Kusong 373-1, Yusong, Taejon, Korea

(Received April 3, 1997; in final form May 12, 1998)

ABSTRACT

The non-uniform moisture distribution in concrete causes the differential drying shrinkage. From this type of differential drying shrinkage, tensile stress occurs on the exposed surface of concrete structures and may result in crack formation. This residual stress is significantly affected by the creep of concrete. In this study, for the purpose of predicting the differential drying shrinkage, the analysis method was suggested, in which the creep of concrete was also considered. In addition, the differential drying shrinkage strain was measured at various positions in concrete by using embedded strain gauges. The internal drying shrinkage strain differs significantly according to the depth from exposed surface. The validity of analysis method was verified by comparing test results with analytical results. Finally it was found that analytical results were in good agreement with test results. © 1998 Elsevier Science Ltd

Introduction

Water in concrete is a very important factor on the material properties of concrete such as drying shrinkage, creep, fire resistance, durability, and freeze-thaw resistance. Thus it is very important to predict the moisture distribution in concrete structures. The water movement within concrete is more complex than other porous media because a very wide range of pore structures are present in cement paste and pore structures change with age.

In the concrete structures exposed to environmental conditions, water movement occurs by moisture diffusion in concrete. Thus the moisture content in concrete varies in both space and time, and the moisture distribution of a cross section of concrete is non-uniform. This non-uniform moisture distribution causes the differential drying shrinkage. From this type of differential drying shrinkage, tensile stress occurs on the exposed surface of concrete structures and may result in crack formation. This residual stress is significantly affected by the creep of concrete.

Therefore, to estimate the differential drying shrinkage, an accurate and general theoretical model for cementitious materials is necessary, but does not exist up to now due to the complexity of the moisture diffusion process in concrete. However, the model based on the

¹To whom correspondence should be addressed.

moisture diffusion proposed by Bazant has been widely used for moisture diffusion analysis (1). Therefore, using the analytical results of moisture distribution, an attempt has been made to consider the effect of moisture distribution on concrete structures (2–4).

The purpose of this study is to predict the differential drying shrinkage in concrete. The analysis method for differential drying shrinkage was suggested, in which the creep of concrete was considered. The differential drying shrinkage strain was also measured at various positions in concrete by using the embedded strain gauges, and then test results were compared with analytical results.

Moisture Diffusion in Concrete

The moisture flux (J) is proportional to the gradient of the pore relative humidity, and is expressed as Eq. 1:

$$J = -k \text{ grad } h \quad (1)$$

where h is the pore relative humidity, and k is the permeability. The specific water content (w) is the function of pore relative humidity (h) in the desorption isotherm, i.e., $w = w(h)$, so that the mass balance equation can be expressed as follows:

$$\frac{\partial w}{\partial t} = \frac{\partial w}{\partial h} \frac{\partial h}{\partial t} = \frac{1}{c} \frac{\partial h}{\partial t} = -\text{div } J \quad (2)$$

where $\partial w/\partial h$ is the moisture capacity, which represents the slope of the desorption isotherm. Eliminating w and J from Eqs. 1 and 2, the nonlinear moisture diffusion equation can be obtained as follows:

$$\frac{\partial h}{\partial t} = c \text{ div}(k \text{ grad } h) = \text{div}(D \text{ grad } h) \quad (3)$$

where D is the moisture diffusion coefficient, and defined as $c \cdot k$. The moisture diffusion coefficient is dependent on the relative humidity and temperature. In CEB-FIP('90) model code (6), for isothermal conditions, the moisture diffusion coefficient is expressed as a function of the pore relative humidity $0 < h < 1$ according to Eq. 4:

$$D(h) = D_1 \left(\alpha + \frac{1 - \alpha}{1 + [(1 - h)/(1 - h_c)]^n} \right) \quad (4)$$

where D_1 is the maximum of $D(h)$ for $h = 1.0$, $\alpha = D_0/D_1$, D_0 is the minimum of $D(h)$ for $h = 0.0$, h_c is the pore relative humidity at $D(h) = 0.5D_1$, and n is an exponent. $\alpha = 0.05$, $h_c = 0.80$, and $n = 15$ are approximately assumed (6). D_1 may be also estimated from Eq. 5:

$$D_1 = \frac{D_{1,o}}{f_{ck}/f_{cko}} \quad (5)$$

where $D_{1,o} = 3.6 \times 10^{-6} \text{ m}^2/\text{h}$, $f_{cko} = 10 \text{ MPa}$, and the characteristic compressive strength f_{ck} may be estimated by the mean compressive strength f_{cm} , i.e., $f_{ck} = f_{cm} - 8 \text{ MPa}$.

As the boundary condition of moisture, it is necessary to correlate the surface moisture

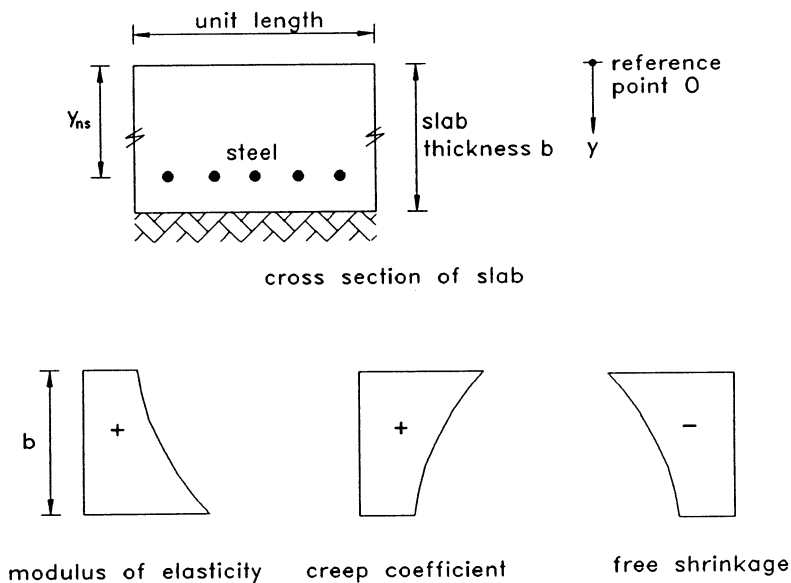


FIG. 1.

Variation of material properties in cross section of slab.

with the humidity of the environmental atmosphere. On the exposed surface S , the boundary condition is as follows.

$$D \left(\frac{\partial h}{\partial n} \right)_S = f(h_{en} - h_s) \quad (6)$$

where f is the surface factor, h_{en} is the environmental humidity, and h_s is the relative humidity on the exposed surface. Bazant dealt with this problem by assuming an additional thickness to the specimen, i.e., the equivalent surface thickness (1). Comparing analytical results with experimental ones, Bazant reported that the value of the equivalent surface thickness is 0.75 mm.

In this study, Eq. 3 is formulated by the finite element method considering the boundary condition in Eq. 6 (7). However, the details are not given in this paper.

Analysis for Differential Drying Shrinkage of Concrete

Figure 1 represents the concrete slab in which one-dimensional moisture diffusion occurs. Due to the moisture diffusion at drying, the moisture distribution in a cross section of slab is non-uniform, and the moisture difference at each location of the concrete causes the variation of material properties, such as modulus of elasticity, creep coefficient, and free shrinkage. Thus the cross section of slab is internally restrained, so that a tensile stress is induced at the exposed surface and a compressive stress in the core of the slab. If this tensile stress on the exposed surface exceeds the concrete strength, surface cracks may be also occurred.

In this study, the analysis method for differential drying shrinkage is suggested, in which

the creep of concrete is considered. The analysis method is satisfied with the equilibrium and compatibility condition, and the differential drying shrinkage is quantitatively calculated. Furthermore, the analysis is accomplished in small time steps.

Free Shrinkage of Concrete

The relationship between shrinkage and pore relative humidity at each location of concrete is important to estimate the differential drying shrinkage. The free shrinkage strain is not directly measured, and is properly modeled as a function of pore relative humidity. In this study, the free shrinkage strain of concrete is approximately described as Eq. 7 (8):

$$\Delta \epsilon_{sh}(t, t_0) = k_{sh} f_s(h) = k_{sh}(1 - h) k_{sh} = \epsilon_s^0 g_s(t) \quad (7)$$

where k_{sh} is the shrinkage coefficient, ϵ_s^0 is the ultimate drying shrinkage on complete drying, and $g_s(t)$ is the ratio of elastic modulus with time, i.e., $g_s(t) = E(t_0)/E(t)$.

Creep of Concrete

Additional creep due to drying (drying creep) is essentially stress-induced shrinkage (8) and should be considered in the analysis for differential drying shrinkage. In this study, stress-induced shrinkage is calculated by the simple equation described by Bazant in Ref. (9). It is known that the microcracking effect also contributes to drying creep (8). However, it is neglected for simplification in this study.

This drying creep is taken into account separately in the form of stress-induced shrinkage. Thus when a stress increment changes from zero at time t_0 to a final value $\Delta \sigma_c(t, t_0)$ at time t , the total strain for elastic and creep deformations of concrete is as follows:

$$\Delta \epsilon_c(t, t_0) = \frac{\Delta \sigma_c(t, t_0)}{E_c(t_0)} [1 + \chi \phi(t, t_0)] + \Delta \epsilon_{cs}(t, t_0) = \frac{\Delta \sigma_c(t, t_0)}{\bar{E}_c(t, t_0)} + \Delta \epsilon_{cs}(t, t_0) \quad (8)$$

where $\Delta \epsilon_{cs}(t, t_0)$ is the stress-induced shrinkage, and χ is the aging coefficient, which is generally about 0.8 (10).

Analysis for Differential Drying Shrinkage

For a reinforced concrete section, the combination of the axial force (N) and bending moment (M) is equivalent to the axial force at reference point O in Figure 1 and the combined bending moment, i.e., the equivalent axial force (N_{eq}) and equivalent bending moment (M_{eq}). Thus the instantaneous strain ($\epsilon_o(t_0)$) at reference point O and curvature ($\psi(t_0)$) at time t_0 are given by Eq. 9:

$$\begin{Bmatrix} \epsilon_o(t_0) \\ \psi(t_0) \end{Bmatrix} = \frac{1}{E_c(t_0)(AI - B^2)} \begin{bmatrix} I & -B \\ -B & A \end{bmatrix} \begin{Bmatrix} N_{eq} \\ M_{eq} \end{Bmatrix} \quad (9)$$

where A , B , and I are respectively the area, first, and second moment of the transformed section about an axis through the reference point O. $E_c(t_0)$ is the modulus of elasticity of concrete at time t_0 .

The instantaneous strain and stress in concrete section at time t_0 are as follows:

$$\varepsilon_c(t_0) = \varepsilon_o(t_0) + \psi(t_0)y \quad (10)$$

$$\sigma_c(t_0) = E_c(t_0)[\varepsilon_o(t_0) + \psi(t_0)y] \quad (11)$$

The instantaneous stress in steel is also calculated from Eq. 12:

$$\sigma_{ns}(t_0) = E_{ns}[\varepsilon_o(t_0) + \psi(t_0)y_{ns}] \quad (12)$$

where E_{ns} is the modulus of elasticity of steel.

At time t , if the moisture distribution in concrete is non-uniform, the restraining force ($\Delta\sigma_r$) is introduced at each location of concrete. And the strain change due to differential drying shrinkage and creep is restrained. Thus the strain increment due to differential drying shrinkage and creep during time t_0 to t plus the strain due to restraining force is zero. That is, the compatibility condition is satisfied with Eq. 13:

$$\phi(t, t_0)\varepsilon_c(t_0) + \Delta\varepsilon_{sh}(t, t_0) + \frac{\Delta\sigma_r(t, t_0)}{E_c(t_0)} [1 + \chi\phi(t, t_0)] + \Delta\varepsilon_{cs}(t, t_0) = 0 \quad (13)$$

In Eq. 13, the restraining force at each location of the cross section of concrete is obtained as Eq. 14:

$$\Delta\sigma_r(t, t_0) = -\bar{E}_c(t, t_0)[\phi(t, t_0)\varepsilon_c(t_0) + \Delta\varepsilon_{sh}(t, t_0) + \Delta\varepsilon_{cs}(t, t_0)] \quad (14)$$

The resultant forces (ΔN , ΔM) of restraining force are calculated by integrating over the area of cross section, as follows:

$$\begin{aligned} \Delta N &= \int \Delta\sigma_r(t, t_0)dA \\ &= -\varepsilon_c(t_0) \int_0^b \bar{E}_c(t, t_0)\phi(t, t_0)dy - \int_0^b \bar{E}_c(t, t_0)\Delta\varepsilon_{sh}(t, t_0)dy - \int_0^b \bar{E}_c(t, t_0)\Delta\varepsilon_{cs}(t, t_0)dy \end{aligned} \quad (15)$$

$$\begin{aligned} \Delta M &= \int \Delta\sigma_r(t, t_0)y dA \\ &= -\varepsilon_c(t_0) \int_0^b \bar{E}_c(t, t_0)\phi(t, t_0)y dy - \int_0^b \bar{E}_c(t, t_0)\Delta\varepsilon_{sh}(t, t_0)y dy \\ &\quad - \int_0^b \bar{E}_c(t, t_0)\Delta\varepsilon_{cs}(t, t_0)y dy \end{aligned} \quad (16)$$

The opposite forces $-\Delta N$, $-\Delta M$ are applied on the cross section of concrete to remove the restraint. Thus the strain increment ($\Delta\varepsilon_o(t, t_0)$) at reference point O and curvature increment ($\Delta\psi(t, t_0)$) at time t are given by the application of the forces $-\Delta N$, $-\Delta M$ on the cross section of concrete:

$$\begin{Bmatrix} \Delta\varepsilon_o(t, t_0) \\ \Delta\psi(t, t_0) \end{Bmatrix} = \frac{1}{\bar{E}_c(t, t_0)(\bar{A}\bar{I} - \bar{B}^2)} \begin{bmatrix} \bar{I} & -\bar{B} \\ -\bar{B} & \bar{A} \end{bmatrix} \begin{Bmatrix} -\Delta N \\ -\Delta M \end{Bmatrix} \quad (17)$$

TABLE 1
Test variables.

Depth from exposed surface (cm)	2, 5, 8, 12
Compressive strength (MPa)	28, 44

where \bar{A} , \bar{B} , and \bar{I} are respectively the area, first, and second moment of the age-adjusted transformed section about an axis through the reference point O.

Then the strain and stress in concrete section at time t are as follows:

$$\epsilon_c(t, t_0) = \epsilon_c(t_0) + (\Delta\epsilon_o(t, t_0) + \Delta\psi(t, t_0)y) \tag{18}$$

$$\begin{aligned} \Delta\sigma_c(t, t_0) &= \Delta\sigma_r(t, t_0) + \bar{E}_c(t, t_0)[\Delta\epsilon_o(t, t_0) + \Delta\psi(t, t_0)y] \\ \sigma_c(t, t_0) &= \sigma_c(t_0) + \Delta\sigma_c(t, t_0) \end{aligned} \tag{19}$$

The steel stress at time t is calculated from Eq. 20:

$$\sigma_{ns}(t, t_0) = \sigma_{ns}(t_0) + E_{ns}[\Delta\epsilon_o(t, t_0) + \Delta\psi(t, t_0)y_{ns}] \tag{20}$$

Measurement of Differential Drying Shrinkage Strain

Test Variables

As shown in Table 1, the differential drying shrinkage strain of concrete, of which compressive strength of 28 and 44 MPa was selected for the tests, was measured at the distance of 2, 5, 8, and 12 cm from exposed surface.

Materials and Mix Proportions.

The cement used in this test is ordinary portland cement (ASTM Type I), and the fine aggregate is river sand. The crushed granite gravel passing the 19-mm sieve was used as the coarse aggregate. Detailed mix proportions are given in Table 2. A superplastizer which meets ASTM C 494 requirements for Type F admixture is used to obtain good workability in Mix II (w/c = 40%).

TABLE 2
Mix proportions of concrete.

Specimen	w/c (%)	s/a (%)	Unit weight (kg/m ³)				Admixture (c × %)	f'_c (MPa)
			Water(w)	Cement(c)	Sand(s)	Gravel(g)		
Mix I	65	42	202	310	740	1020	—	28
Mix II	40	38	172	430	661	1079	1.0	44

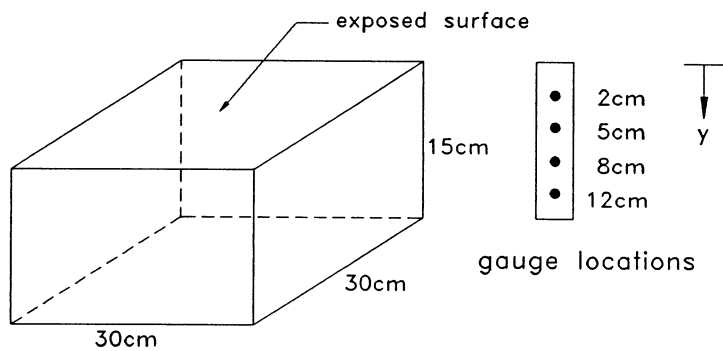


FIG. 2.
Geometry and size of specimen.

Testing Details and Procedure

The differential drying shrinkage was measured by using the embedded strain gauges, and test results were compared with analytical results. The embedded strain gauges were used to measure the internal concrete strain (11). Figure 2 shows the geometry and size of specimen. Five sides of specimen were sealed with paraffin wax to ensure the uniaxial moisture diffusion. The partially sealed specimen of Figure 2 can be regarded as an element of infinite slab that is 30 cm thick and is drying from both faces. The embedded strain gauges were installed at the distance of 2, 5, 8, and 12 cm from exposure surface. After moist-curing for 7 days, specimens were exposed to a constant-temperature and constant-humidity room of $20 \pm 1^\circ\text{C}$ and $68 \pm 2\%$ RH.

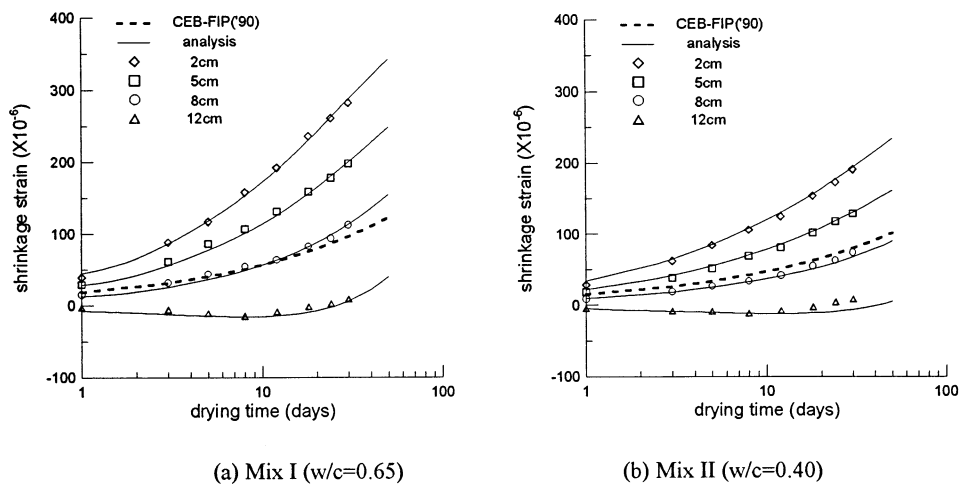


FIG. 3.

Comparison of test results with analytical results of internal drying shrinkage. (a) Mix I (w/c = 0.65); (b) Mix II (w/c = 0.40).

TABLE 3
Input data of moisture diffusion coefficient.

Specimen	D_1 (m ² /h)	α	h_c	n
Mix I	1.81×10^{-6}	0.05	0.80	15
Mix II	1.00×10^{-6}	0.05	0.80	15

Experimental and Analytical Results

Figure 3 shows the test results of the internal drying shrinkage at each location of concrete, i.e., differential drying shrinkage strain. The internal drying shrinkage strain differs significantly according to the depth from exposed surface, and the shrinkage strain is greater at the depth close to exposed surface than an inner region in concrete. In Figure 3, the shrinkage strain near the exposed surface rapidly increases at the early stages of drying, but inside the concrete, shrinkage strain changes very slowly. In Mix I, the difference of shrinkage strain at each location is higher than that of Mix II. This tendency is the same as the difference of the average drying shrinkage of concrete for mix proportions. Thus the differential drying shrinkage must be considered in the analysis of concrete structures. And it seems that the technique using the embedded strain gauges is suitable for measuring the internal shrinkage strain distribution due to non-uniform moisture distribution.

Based on the moisture diffusion equation, the analysis for moisture distribution in concrete of Figure 2 is carried out to analyze the differential drying shrinkage. Input data related to the moisture diffusion coefficient are shown in Table 3. The geometric conditions, mix proportions of concrete, and atmospheric conditions are the same as test conditions.

Then, using the analytical results of moisture distribution, the differential drying shrinkage is analyzed according to the analysis procedure presented above. The creep of concrete is also

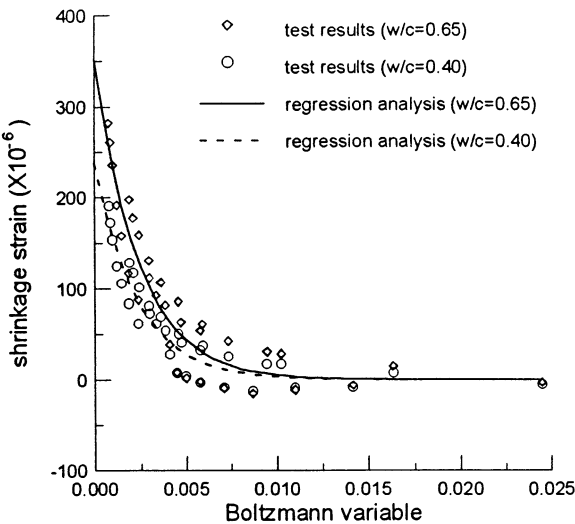


FIG. 4.
Shrinkage strain distribution in time and space.

TABLE 4
Regression coefficients of Eq. 21.

Specimen	a	b	r^*
Mix I	353×10^{-6}	-415.4	0.95
Mix II	238×10^{-6}	-426.1	0.95

r^* : coefficient of correlation

considered in the analysis of differential drying shrinkage. The analytical results are in good agreement with test results. It seems that the differential drying shrinkage is well predicted by this analysis method.

The distribution of internal shrinkage strain is plotted against the Boltzmann variable λ ($\lambda = y/\sqrt{t}$) as shown in Figure 4, where y is the depth from drying surface (m) and t is the drying time (h). Figure 4 clearly shows the distribution of internal shrinkage strain with space and time. From the use of Boltzmann variable, test results can be represented by one variable λ . Finally, test results are fitted as Eq. 21, and the regression coefficients of Eq. 21 are given in Table 4.

$$\varepsilon_{sh}(y, t) = ae^{b\lambda} \quad (21)$$

Conclusions

From the results of this investigation on differential drying shrinkage, the following conclusions can be drawn:

1. The internal drying shrinkage strain significantly varies according to the depth from drying surface, and the stresses induced by this differential drying shrinkage may cause surface cracks. Thus the differential drying shrinkage must be considered in the analysis of thick concrete structures.
2. For the analysis method of differential drying shrinkage, the creep of concrete needs to be considered, and the analytical results obtained by this method were in good agreement with test results.
3. According to the differential drying shrinkage strain measured at various positions of concrete by using the embedded strain gauges, it seems that the technique using the embedded strain gauges is suitable for measuring the internal drying shrinkage strain distribution.

Acknowledgment

The authors gratefully acknowledge the financial support of this work from the Korea Science & Engineering Foundations (ERC-STRESS).

References

1. Z.P. Bazant and L.J. Najjar, Mater. Struct. 5, 3–20 (1972).
2. J.M. Illston and A. Tajirian, Mag. Concr. Res. 29, 175–190 (1977).

3. Z.P. Bazant and W. Thonguthai, *J. Eng. Mech. Div., ASCE*, 104, 1059–1079 (1978).
4. K. Sakata, *Cem. Concr. Res.* 13, 216–224 (1983).
5. Z.P. Bazant and J.K. Kim, *Mater. Struct.* 24, 323–326 (1991).
6. Comité Euro-International du Béton, “CEB-FIP Model Code 1990,” 68–69 (1993).
7. R.M. Polivka and E.L. Wilson, “Finite Element Analysis of Nonlinear Heat Transfer Problems,” University of Berkeley, 1976.
8. Z.P. Bazant and Y. Xi, *Mater. Struct.* 27, 3–14 (1994).
9. Z.P. Bazant, V. Kristek, and J. Vitek, *J. Struct. Eng., ASCE*, 118, 305–321 (1992).
10. A. Ghali and R. Favre, “Concrete Structures—Stresses and Deformations,” E&FN SPON, 1994, pp. 444.
11. R.H. Scott and P.A.T. Gill, *Mag. Concr. Res.* 39, 109–112 (1987).